CNS Drug Disposition:

The Relationship Between *In Situ* Brain Permeability and Brain Free Fraction

Authors: Scott Summerfield, Kevin Read, David J Begley, Tanja Obradovic,

Ismael J Hidalgo, Sara Coggon, Ann V Lewis, Rod A Porter, Phil Jeffrey.

Drug Metabolism and Pharmacokinetics Department, Neurology and Gastrointestinal and Centre of Excellence for Drug Discovery, GlaxoSmithKline R&D, New Frontiers Science Park, Third Avenue, Harlow, Essex, CM19 5AW (SGS, VAL, PJ).

Department of Medicinal Chemistry, Psychiatry Centre of Excellence for Drug Discovery, GlaxoSmithKline R&D, New Frontiers Science Park, Third Avenue, Harlow, Essex, CM19 5AW (RP).

Drug Metabolism and Pharmacokinetics Department, Psychiatry Centre of Excellence for Drug Discovery, GlaxoSmithKline R&D, Via A. Fleming 4, Verona, Italy, 37135 (KR).

Kings College London, Pharmaceutical Sciences Research Division and Wolfson Centre for Age-related Disease, Hodgkin Building, Guys Campus, London, SE1 1UL, UK (DB).

Absorption Systems, 440 Creamery Way, Suite 300, Exton, PA 19341 (TO, IJH).

Drug Metabolism and Pharmacokinetics Department, UCB Celltech, Granta Park, Great Abington, Cambridge, CB1 6GS, United Kingdom (SC).

Relationship between Permeability and Brain Free Fraction

Corresponding author: Scott Summerfield, Drug Metabolism and Pharmacokinetics Department, Neurology and Gastrointestinal Centre of Excellence for Drug Discovery, GlaxoSmithKline R&D, New Frontiers Science Park, Third Avenue, Harlow, Essex, CM19 5AW.

Tel: +44 (0)1279 627926

Fax +44 (0)1279 622727

Email: Scott.G.Summerfield@GSK.com

Abbreviations: BBB, blood-brain barrier; Papp, apparent membrane permeability; fu(brain), *in vitro* free fraction in brain tissue ; P, *in situ* brain permeability; MDR1-MDCKII, Madin Darby Dog Kidney type II cells expressing the human MDR1 gene for P-gp.

No. text pages: 23

No. references: 40

No. tables: 1

No. figures: 6

No. words (Abstract): 138

No. words (Introduction): 713

No. words (Discussion): 1480

Abstract

The dispositions of 50 marketed CNS drugs into the brain have been examined in terms of their rat *in situ* permeability (P) and *in vitro* permeability (Papp) alongside lipophilicity and free fraction in rat brain tissue. The inter-relationship between these parameters highlights that both permeability and brain tissue binding influence the uptake of drugs into the CNS. Hydrophilic compounds characterised by low brain tissue binding display a strong correlation ($R^2 = 0.82$) between P and Papp, whereas the uptake of more lipophilic compounds appears to be influenced by both Papp and brain free fraction. A non-linear relationship is observed between $logP_{oct}$ and P over the 6 orders of magnitude range in lipophilicity studied. These findings corroborate recent reports in the literature that brain penetration is a function of both rate and extent of drug uptake into the CNS.

Introduction

The development of new drugs targeting the central nervous system (CNS) is the fastest growing franchise within the pharmaceutical sector, although this growth has been tempered by relatively poor success of novel candidates (Alavijeh *et al.*, 2005). One of the significant challenges in treating CNS conditions is drug passage across the blood-brain barrier (BBB), a layer of endothelial cells connected with tight junctions that express numerous drug metabolising enzymes and efflux transporters (Pardridge, 1997; Tamai and Tsuji, 2000). Therefore, investigation of drug properties that are favourable for CNS delivery can greatly improve efforts in Drug Discovery.

A number of methods are available to determine the rate of uptake of drugs from blood into brain parenchyma (Begley, 1999). In the pharmaceutical industry, CNS penetration is usually assessed in rodents following either intravenous or oral dosing to determine the brain to blood concentration ratio. This takes into account not only BBB penetration but also binding, metabolism and clearance. However, there can be marked species differences in the influence of these parameters on overall BBB penetration; hence there is significant value in removing some of this complexity and assessing brain penetration at the level of the BBB *in situ*. Considering that the BBB is conserved across species (Cserr and Bundgaard, 1984) this may represent a more meaningful indicator of the intrinsic ability of the compound to cross the BBB in man. Furthermore, *in situ* techniques offer an ideal validation tool for assessing *in vitro* BBB models and also provide further insight into the molecular descriptors which are crucial for BBB penetration.

Brain perfusion has been used in neurochemical research for over 50 years. Early methods focused on long term perfusion of isolated brain and required extensive surgical preparation (Woods and Youdim, 1978). Then, in the 1980's the development of the *in situ* rat brain perfusion technique (Takasato *et al.*, 1984), provided a simple method for performing short term studies of brain uptake following less complex surgery. Several variants have been published that modify and extend the original method, including those of Greenwood et al. (1985) and Zlokovic et al. (1986). The *in situ* brain perfusion method involves cannulation of the carotid artery and infusing whole blood, physiological buffer or saline containing the compound of interest. Because of the possibility of extending perfusion time, this model allows transport studies of slowly penetrating and metabolically unstable, drugs. Furthermore, because there is complete control over perfusate composition, perfusate flow and perfusion time, investigation of other variables is possible, including plasma protein binding or the influence of specific drug transporters. There are many examples in the literature of the successful application of *in situ* brain perfusion to study the CNS uptake of compounds (Takada *et al.*, 1992; Chickhale *et al.*, 1995). Comparisons have been made with results obtained with *in vitro* models of the BBB (Pardridge *et al.*, 1990; Chickhale *et al.*, 1994) and *in situ* perfusion data has also been used to refine or develop predictive computational models of BBB permeability (Liu *et al.*, 2004).

Reports have shown that drug permeation into the CNS is influenced by physicochemical properties as well as the potential to interact with transport systems at the BBB. It has been suggested that the optimal molecular weight for passage into the brain lies in the region of 300 – 400 Da (Fisher *et al.*, 1998), ideally with low

polar surface area ($< 80\text{Å}^2$, Clark, 1999), and permeability into the CNS (Takasato *et al.*, 1984). However, previous investigations have been performed on a limited number of compounds, many of which are not therapeutic agents (Murakami *et al.*, 2000; Takasato *et al.*, 1984). In this work brain disposition of 50 CNS marketed drugs has been investigated, covering a wide range of physicochemical characteristics. The present study investigated relationship between drug *in situ* brain permeability product (P), lipophilicity (clogP$_{oct}$), *in vitro* permeability (Papp) across MDR1-MDCKII cell monolayers (Mahar Doan *et al.*, 2002; Wang *et al.*, 2005), and the unbound drug fraction in rat brain tissue, a parameter recently reported to influence CNS penetration (Kalvass and Maurer, 2002). Over a cLogP$_{oct}$ range of ca. 0 to 6, there is a non-linear relationship observed between lipophilicity and P. In addition, P appears to be influenced not only by the drug permeability across the BBB, but also by binding to brain tissue.

Materials and Methods

Chemical structures for the 50 compound set are supplied in Supplemental File 1.

The following compounds were obtained from commercial sources; Risperidone,

Chlorpromazine, Bupropion, Pergolide Mesylate, Amitryptiline, Diazepam,

Meprobamate and Temazepam (Sigma Chemical Company, Poole, Dorset, UK);

Venlafaxine, Citalopram, Pemoline and Midazolam (Sequoia Research Products Ltd,

Oxford, United Kingdom). All other compounds were available from in house

sources.

Calculated Physicochemical Properties

Log octanol/water partition coefficients (clogP$_{oct}$) were calculated using CLOGP

software, Biobyte Corporation, Claremont, California. Calculation of Polar surface

area (PSA) was based on the work of Clark (1999).

Equilibrium Dialysis Measurements

96-well equilibrium dialysis apparatus was used to determine the free-fraction in the

blood and brain for each drug (HT Dialysis LLC, Gales Ferry, CT, USA).

Membranes (3kDA cut-off) membranes were conditioned in deionized water for 40

min, followed by conditioning in 80:20 deionised water:ethanol for 20 min, and then

rinsed in deionised water before use. Rat brains were obtained fresh on the day of the

experiment and were homogenised with PBS to a final composition of 1:2 brain:PBS,

by means of ultrasonication (Tomtec Autogiser, Receptor Technologies, Adderbury,

Oxon, UK) in an ice bath. Diluted brain homogenate was spiked with the test

compound (1000 ng/g) and 100-µl aliquots (n = 6 replicate determinations) were

loaded into the 96-well equilibrium dialysis plate. Dialysis versus PBS (100 uL) was

7

carried out for 5h in a temperature controlled incubator at 37°C (Stuart Scientific, Watford, UK), using an orbital microplate shaker at 125 rev/min (Stuart Scientific, Watford, UK). At the end of the incubation period, aliquots of brain homogenate or PBS were transferred to Matrix ScreenMate tubes (Matrix Technologies, Hudson, NH, USA), and the composition in each tube was balanced with control fluid such that the volume of PBS to brain was the same. Sample extraction was performed by the addition of 200 uL of acetonitrile containing an internal standard. Samples were allowed to mix for 15 minutes and then centrifuged at 2465 x g in 96-well blocks for 20 min (Eppendorf 5810R, VWR International, Poole, Dorset, UK). The unbound fraction was determined as the ratio of the peak area in buffer to that in brain, with correction for dilution factor according to equation 1 (Kalvass and Maurer, 2002).

$$fu = \frac{(1/D)}{\{[1/fu(apparent)]-1\}+1/D\}} \qquad (1)$$

where, D = dilution factor in brain homogenate and fu(apparent) is the measured free fraction of diluted brain tissue.

MDR1-MDCKII Cell Passive Membrane Permeability Measurements

Cell culture media, bovine serum albumin, medium supplements (L-glutamine, 20 mM sodium bicarbonate, non-esential amino acids, sodium pyruvate, colchicine), Hanks' balanced salt solution (HBSS) was purchased from Invitrogen (Carlsbad, CA). Transwells (12-well, 1.13 cm^2 area, 0.4 µm pores) were purchased from Costar (Cambridge, MA). Krebs Ringer Bicarbonate buffer was obtained from Sigma-Aldrich (St Louis, MO) and drugs were supplied by GlaxoSmithKline (UK).

Multi-Drug Resistance Madin-Darby Canine Kidney (MDR1–MDCK) type II cells were obtained from NIH (National Institute of Health) (Bethesda, MD). Cells were maintained in minimum essential Eagle's medium containing 2 mM L-glutamine, 20 mM sodium bicarbonate, 0.1 mM non-essential amino acids, 1 mM sodium pyruvate, and 10 % bovine serum albumin supplemented with 0.2 mM colchicine to maintain P-gp expression. For permeability experiments, cells with passage numbers 24-33 were seeded at a density of 60,000 cells/cm^2 on rat type I collagen-coated polycarbonate membranes in 12-well transwell plates. The experiments were performed on the 8th day after seeding. Prior to the permeation assay, the transepithelial electrical resistance (TEER) was measured on each cell monolayer using an Endohm Voltameter (World Precision Instruments, Sarasota, FL). The MDR1-MDCK cell systems used in transport experiments had a high TEER value ranging from 1800 to 2000 Ω cm^2, which differs from lower TEER MDR1-MDCK models often employed in CNS screens (Braun et al, 2000). The permeability assay buffer was Hank's balanced salt solution containing 10 mM HEPES and 15 mM glucose at pH 7.4. The cells were dosed on the apical side and basolateral side, incubated at 37 ^{0}C with 5% CO_2 and 90% relative humidity under shaking conditions (150 rpm) in order to reduce the influence of the unstirred water layer. The test compounds were prepared to a final concentration of 3 µM. In the P-gp inhibition assays, the cells were incubated with 2 µM GF 120918A, a known P-gp inhibitor. Drug permeation was tested in two directions, apical-to-basolateral (A-to-B) and basolateral-to-apical (B-to-A), in triplicate. Sampling was done 60 minutes after dosing. The apparent permeability coefficient (Papp), was calculated as follows:

$$Papp = \frac{dCr}{dt} \bullet \left(\frac{Vr}{A \cdot Co} \right) \qquad\qquad (2)$$

9

where, dC_r/dt is the slope of the cumulative concentration in the receiver

compartment versus time in $\mu M/s^{-1}$; A is the area of the cell monolayer; C_0 is the

drug concentration in the dosing solution. The recovery of most compounds exceeded

80%.

Rat in-situ Brain Perfusion Model

The *in situ* rat brain perfusion procedure was similar to that previously described

(Smith *et al.*, 1996). Adult male Sprague-Dawley rats (300 – 350 g) were purchased

from Hilltop Labs (Scottdale, PA, USA). Animals were housed in a temperature

controlled animal facility at West Chester University, PA, USA. All of the

procedures were approved by the Institutional Animal Care and Use Committee of

West Chester University, PA, USA, and conducted in accordance with approved

standards for laboratory animal care.

The rats were anesthetized with a solution containing 50 mg/kg ketamine and 3 mg/kg

xylazine. The left common carotid artery was cannulated with a polyethylene-60

catheter (BD Biosciences, Sparks, MD), which was inserted into the left internal

carotid artery for perfusion. The perfusion fluid consisted of Krebs Ringer

Bicarbonate buffer (KRB) pH 7.4 and was oxygenated with a mixture air of 95% O_2

and 5% CO_2 before starting the perfusion. The perfusion was started immediately

after the cardiac blood supply was cut-off. The perfusion flow rate was 20 ml/min and

perfusate contained one of the compounds (5 - 50 µM). In addition, perfusate also

contained the intravascular space marker atenolol (50 µM) (Street *et al.*, 1979), and a

moderate brain permeability marker, antipyrine (5 µM) (Wang *et al.*, 2005). Each

compound was perfused in 3 animals. Following 30 seconds perfusion, brains were

10

quickly removed from the skull and the left cerebral hemisphere was excised. The

isolated left brain tissue was homogenized in 4 mL of a methanol/water mixture. The

resulting homogenates were stored at –80ºC until analysis.

Calculation of *In Situ* Brain Permeability

The unidirectional transfer constant K_{in} (ml/min/g) and brain permeability P (cm/s)

were determined using the following equation for the single-point perfusion assay:

$$\frac{C_{br}(T)}{C_{pf}(T)} = K_{in}t + V_i \tag{3}$$

and $P = K_{in}/S$ (4)

where C_{br}/C_{pf} is the apparent brain distribution volume, C_{br} is the amount of drug in

the brain tissue (ng of drug /g of brain tissue), C_{pf} is the drug concentration in the

perfusion fluid (ng of drug/ml of fluid), t is the net perfusion time and S is the

luminal area of the brain vascular space (taken as 150 cm^2/g, (Fenstermacher *et al*.,

1988). To compensate for the drug contained in the capillary vascular space from the

brain parenchymal concentration values, the apparent brain distribution volume for

atenolol was subtracted from the drug values in each animal. The apparent vascular

space volume in this study was 11.5 ± 1.4 µL/g of brain tissue (average ± STD,

N=150 animals), which is in good agreement with the sucrose intravascular volume

reported by Smith *et al*. (1988).

Analysis of Test Compounds.

The analytical conditions for *in situ* perfusion experiments were performed at Absorption Systems as follows. Samples were introduced into the mass spectrometer by injecting 10 µL of sample through either a Perkin Elmer (Wellesley, MA) Series 200 HPLC system comprised of an autosampler and two micropumps, or on a Leap Technologies (Carrboro, NC) HPLC system comprised of a FLUX Instruments quaternary pump and a CTC Analytics HTC PAL autosampler. Chromatography was conducted in the reverse-phase mode on either a BDS Hypersil C_{18}, 30 x 2.1 mm column (3 µm; Thermo-Hypersil Keystone; Bellefonte, PA), an AQUASIL C_{18}, 30 x 2.1 mm column (3 µm; Thermo-Hypersil Keystone; Bellefonte, PA), or on a Capcell Pak MF C_8, 50 x 2.0 mm column (5mm; Phenomenex; Torrance, CA). The aqueous mobile phase consisted of 10% 25 mM ammonium formate buffer at pH 3.5 and 90% water. The organic mobile phase consisted of 10% 25 mM ammonium formate buffer at pH 3.5 and 90% acetonitrile. Analytes were eluted using a gradient of aqueous and organic mobile phase at a flow rate of 300 µL/min. Determination of all analytes was performed by LC-MS/MS detection. Analysis was performed on type API3000 or API4000 triple quadrupole mass spectrometers purchased from Applied Biosystems (Foster City, CA), equipped with an electrospray (ESI) source at 450ºC, and operated in the MRM (MS/MS) mode. Mass spectrometer parameters were individually optimized for each analyte. Typical run times ranged from 3.5 to 4.5 minutes and the optimised HPLC/MS/MS are supplied in Supplementary File 2.

The analytical conditions for equilibrium dialysis experiments were performed at GlaxoSmithKline as follows. All samples were analysed by means of HPLC/MS/MS on a PE-Sciex API-4000 tandem quadrupole mass spectrometer (Applied Biosystems,

Ontario, Canada), employing a Turbo V Ionspray operated at a source temperature of 700°C (80 psi of nitrogen). Samples (3-10 µl) were injected using a CTC Analytics HTS Pal autosampler (Presearch, Hitchin, UK) onto a Hypersil Aquastar 3.0 x 30 mm, 3-µm column (Thermo, Runcorn, Cheshire, UK) operated at 40°C and at an eluent flow rate of 1 mL/min. Analytes were eluted using a high-pressure linear gradient program, by means of an HP1100 binary HPLC system (Agilent, Stockport, Cheshire, UK), using acetonitrile as solvent B. For HPLC/MS/MS analysis in positive ion mode solvent A comprised 1mM ammonium acetate containing 0.1% (v/v) formic acid, while in negative ion mode solvent A comprised 1 mM ammonium acetate. The gradient was held at 5% solvent B for 2 min, before increasing to 90% at 1.2 min, remaining at 90% until 1.6 min before returning to the starting conditions. The cycle time was 2.5 min per sample. Relative peak areas between the PBS and tissue half-wells were used to determine the respective free fractions. Typical run times ranged from 3.5 to 4.5 minutes and the optimised HPLC/MS/MS in Supplementary File 3.

Results

The compounds selected in this study comprised 50 drugs marketed for CNS

indications, covering a wide range of physicochemical properties and chemical space.

These properties vary as follows; molecular weight (136 – 582 Da, median 306 amu),

lipophilicity (clogP$_{oct}$ -0.2 – 6.1, median 3.0) and polar surface area (3 – 118, median

38). Hydrogen bond acceptors range between 0 and 5 while hydrogen bond donors

range between 0 and 3. Since all of the 50 drugs have been employed to treat

conditions of the CNS, this compound set represents a composite profile of

physiochemical properties that are required to facilitate drug disposition into the brain

and achieve therapeutic concentrations.

For most CNS drugs that act directly at targets within brain tissue, it is a requirement

for these molecules to first cross the BBB in order to elicit a therapeutic effect. No

single factor dictates their CNS uptake, although lipophilicity does appear to exhibit a

strong influence on this process (Table 1). The role of lipophilicity was examined

against three CNS related parameters, fu(brain) (Figure 1a), apical-to-basolateral

passive membrane permeability across a cell monolayer, measured in the presence of

the P-gp inhibitor, elacridar (Figure 1b) and *in situ* brain permeability (P, Figure 2).

The Influence of Lipophilicity on fu(brain), Papp and P

Figure 1a shows that the unbound fraction in brain tissue decreases markedly with

increasing lipophilicity (Figure 1a), varying over 1000-fold from trifluoperazine

(cLogP$_{oct}$ 5.1, fu(brain) = 0.0007) to ethosuximide (cLogP$_{oct}$ 0.4, fu(brain) = 0.73).

There is, however, a notable degree of scatter in the correlation of cLogP$_{oct}$ and

fu(brain). Although measured lipophilicity data was generated on a subset of these

14

compounds (logD and CHI logP, data not shown), no improvement was noted over *in silico* estimates. In part this degree of scatter may be related to the fact that $cLogP_{oct}$ assesses partitioning from the aqueous phase into octanol whereas the composition of brain tissue (either homogenate or slice) is appreciably more complex than this aliphatic alcohol. Despite this, there does appear to be a general trend toward a reduction in fu(brain) with increasing lipophilicity, and a similar observation has been noted for lead optimisation compounds being screened in the current drug discovery paradigm (Summerfield *et al.*, 2006).

In the case of passive membrane permeability there is a non-linear relationship noted between $cLogP_{oct}$ and Papp (Figure 1b). Papp values range from $0.4 - 55 \times 10^{-6}$ cm/s across the compound set and there appears to be an inverted U-shape distribution in Papp over the 6 order of magnitude range in lipophilicity. Papp values appear to attain a plateau around $clogP_{oct}$ 2 to 4, indicating an optimum range of values for transfer across the cell monolayer. This parabolic inverted "U" distribution is reminiscent of the *in vivo* hypnotic effect of barbiturates where the maximum *in vivo* effect is obtained at a $LogP_{oct}$ of ~2 (Hansch *et al.*, 1967). Increasing hydrophobicity and hydrophilicity both result in a reduction of the hypnotic effect, highlighting the possibility that similar factors may influence drug distribution and activity (in both *in vivo* and *in vitro* systems) when there are aqueous phases on either side of a barrier. To reduce the influence of the unstirred water layer gentle agitation was applied to the MDR1-MDCKII incubations. In addition correction for the unstirred layer using antipyrine as a reference yield no change in the trends observed.

Lipophilicity and its relationship to *in situ* brain permeability are examined in Figure

2. In this study brain perfusions were performed over a 30 second period to ensure

that the Kin values were determined on the linear region of the brain uptake curve.

This also facilitated the analysis of a large set of compounds (n = 50) in order to

examine trends across a wide lipophilicity range. Brain permeability was calculated

by normalising Kin for the luminal area of the brain vascular space, which gives

comparable units to the *in vitro* Papp values measured for each compounds (i.e. cm/s).

Similar units for P and Papp were considered more appropriate for subsequent data

analysis (Figure 4b). Converting Kin to permeability surface product (PS) *via* the

Crone-Renkin equation yields comparable correlations to those presented for P. The

flow component was taken as the highest Kin measured (Sertraline, data not shown).

The perfusion fluid contained the analyte of interest in addition to two reference

compounds; atenolol as a marker of vascular volume and antipyrine as an indicator of

perfusate flow and relatively free unrestricted passive transfer through the endothelial

cell membrane. From the atenolol brain concentration measurements, the vascular

volume was consistent across all animals in the study (11.5 ± 1.4 uL/g, n = 150),

while the P of antipyrine ($1.7 ± 0.03 \times 10^{-3}$ cm/s, n = 150) was similar to that

determined elsewhere (Ohno *et al.*, 1979).

The CNS drug set used in this analysis covers a wider range of lipophilicity (6 orders

of magnitude), with 75% of the compounds being characterised by $cLogP_{oct}$ values in

excess of 2. Figure 2 shows that P displays a non-linear relationship with $clogP_{oct}$,

characterised by a linear portion ($cLogP_{oct}$ < 2 - 3) and a plateau region ($cLogP_{oct}$ > 2 -

3). Furthermore above a $clogP_{oct}$ of approximately 3, most of the compounds are

16

characterised by P values between 15 and 30 x 10^{-3} cm/s; this includes diazepam (P = 13.2 x 10^{-3} cm/s). Previous studies have highlighted a good correlation ($R^2 > 0.9$) between octanol-water partition ratios and P, although these assessments were generally restricted to compounds where the $logP_{oct}$ was less than 2 (for review see Smith *et al.*, 1996). Similarly in this analysis some correlation is noted between lipophilicity and P below a $clogP_{oct}$ of 2. The plateau effect noted in Figure 2 would suggest that the uptake of these lipophilic drugs may due to flow limited distribution into the brain during the *in situ* perfusion, i.e. the rate of brain penetration is maximal. One notable outlier is Lamotrigine (P = 0.84 x 10^{-3} cm/s, $cLogP_{oct}$ = -0.2), which is characterised by a higher P than would be expected from the compounds lipophilicity. In human subjects lamotrigine has been shown to freely pass into the brain with a mean brain:serum ratio of 2.8:1 (Meyer *et al.*, 1999). None of the physicochemical properties examined would indicate this behaviour, while no evidence is available for active brain uptake. Further analysis of lamotrigine is required.

No clear difference in P is observed between P-gp substrates and P-gp non-substrates. This is in contrast to previous reports that P-gp substrates showed reduced PS values relative to non-substrates for a given lipophilicity (Youdim *et al.*, 2004). Generally, however, these reports have used radiotracers for the determination of P whereas this study employed HPLC/MS/MS analysis, which requires higher analyte concentrations (5000 – 50000 pmol/uL) relative to radiodetection. Hence the similarity of P-gp substrates and non-substrates in this study is likely to be a function of the higher perfusion concentrations and a possible partial or complete saturation of the efflux transporter.

The Influence of Passive Membrane Permeability and fu(brain) on P

Figure 3 examines the relationship between P and Papp in which two differing groups of behaviour are defined, group A and B. In group A, P lies in the region of 10 - 15 x 10^{-3} cm/s and is relatively insensitive to changes in Papp over the range 1 – 50 x 10^{-6} cm/s. For group B, P increases in proportion to Papp over the 1 – 50 x 10^{-6} cm/s range. A rationale for this behaviour becomes apparent when lipophilicity is factored into the plot (Figure 3). Group A appears to be comprised of largely lipophilic compounds ($clogP_{oct} > 3$) whereas group B is largely comprised of the less lipophilic drug molecules ($clogP_{oct} < 3$). This suggests that multiple parameters need considering in order to rationalise the magnitude of P.

Since the CNS compartment comprises both the BBB and the brain parenchyma it is possible that drug uptake into the brain is a composite function of both permeability across the BBB and binding to brain tissue. Figures 4a and 4b consider the inter-relationship between P, Papp, $clogP_{oct}$ and fu(brain). Here Papp has been employed as a surrogate for the intrinsic passive permeability across the BBB in the absence of tissue binding. In an attempt to factor out the influence of passive permeability across the BBB, a hybrid term has been employed in this analysis, P/Papp. Against lipophilicity there is a rather weak correlation with P/Papp ($R^2 = 0.45$), however, this is improved markedly by the comparison with fu(brain), ($R^2 = 0.74$, Figure 4b). This raises the possibility that P may be influenced not only by intrinsic BBB permeability (with Papp employed as a surrogate in this analysis) but also the drugs affinity for brain tissue. The classical view of brain permeability would suggest that due to the short time frame of the perfusion (30 s), the brain acts as an infinite sink with respect

to distribution. Under this assumption the rate of drug transfer across the BBB would then be the dominant factor. Figure 4b offers the alternative hypothesis that even at short perfusion times binding to brain tissue acts as a sink to help drive CNS uptake. Again, the P-gp substrates are distributed evenly around the regression line, indicating that this transporter is not influencing P under these experimental conditions.

Despite the correlation noted in Figure 4b, there are four outliers to the trend, namely, fluphenazine, isocarboxid, phenelzine and ziprasidone. The reason for the discrepancy in this correlation is not clear and based on their physicochemical properties they do not form a homogenous group. One possibility is the existence of active uptake since, for example, fluphenazine has been found to interact with the brain glucose transporter (Ardizzone *et al.*, 2001). Excluding these points from the regression analysis would lead to a further improvement in the correlation ($R^2 = 0.87$), but more analysis is required to understand these outliers.

Despite the overall nonlinear relationship highlighted in Figure 2 between $cLogP_{oct}$ and P, there does appear to be a more a linear region for drugs characterised by a $clogP_{oct}$ below *ca.* 2. The low lipophilicity of these drugs results in a low degree of brain tissue binding and under these circumstances it may be expected that passive membrane permeability across the BBB would have a greater influence on the magnitude of P, rather than fu(brain). Indeed this appears to be the case (Figure 5) when fu(brain) is greater than 0.1 ($R^2 = 0.82$), although gabapentin has been excluded as an outlier from this correlation. The lipophilicity of gabapentin ($clogP_{oct}$ 1.2) would suggest a lower P values than observed (1.1 cm/s), although this may be due to

active transport at the level of the BBB (Uchino *et al.*, 2002). Incorporating

additional compounds with lower fu(brain) leads to a rapid deterioration in the

correlation coefficient between P and Papp, suggesting a progressively important and

influential role for the extent of brain tissue binding.

In summary, P may be influenced not only by the permeability across the BBB but

also the affinity of a given drug for brain tissue, particularly where tissue binding

begins to increase (fu(brain < 0.1). It is clear that there are outliers to this correlation

(Figure 4b) along with some variance not accounted for. These factors require further

study.

Discussion

Drug delivery to targets within the brain represents a major obstacle in the development of CNS drugs, since over 98 % of all new candidates do not cross the BBB efficiently (Terasaki and Pardridge, 2000). For that reason, significant efforts have been made to elucidate the factors that influence drug permeation across the BBB and to develop predictive ADME models early in drug discovery (Fisher *et al.*, 1998; Mahar Doan *et al.*, 2002; Wang *et al.*, 2005). This analysis comprises a set of compounds spanning a wide range of both physicochemical properties and targets within the CNS. Lipophilicity ranges 6 orders of magnitude, which is representative of the distributions noted in previous reviews of the properties for a variety of marketed CNS drugs (Bodor and Buchwald, 2003). In terms of P measurements, however, this current study greatly increases the number of compounds assessed above a $logP_{oct}$ of 2 and provides new insights on the inter-relationship between BBB permeability and tissue binding within the brain.

The fraction of free drug available within the brain extracellular fluid is clearly seen to depend on lipophilicity, differing up to a 1000-fold between the most hydrophilic and lipophilic compounds in the test set. Hansch *et al.* (1967) were among the first to use the octanol-water partitioning system to represent the two extremes of the biophase and this scale of lipophilicity has been invaluable in understanding the trends in biological activity and ADME properties. The use of 1-octanol lends itself well to the high throughput assessment of drug partitioning but does represent a great simplification in terms of the composition of the biophase compartment, or brain tissue in this instance. This can be seen in Figure 1a where the correlation of $clogP_{oct}$ and fu(brain) can show marked scatter and also in Figures 4a and 4b where the

relationship with P and Papp is improved with the use of fu(brain) over clogP$_{oct}$. In this instance octanol-water partitioning provides a first approximation to the *in vivo* situation, while binding in brain tissue homogenate is more representative of intact tissue.

The influence of lipophilicity also highlights an intriguing difference between the permeability measured either *in vitro* (Papp) or *in vivo* (P). In terms of Papp there appears to be an inverted U-shape distribution with increasing lipophilicity, showing a plateau around a clogP$_{oct}$ of 2 to 4. These results are in accordance with a previous indication that drug membrane permeation is not proportionally elevated with respect to increases in lipid solubility (Cohen *et al.*, 1972). In the *in situ* paradigm, P shows a similar trend when clogP$_{oct}$ is less than 4 although the plateau extends to higher lipophilicities (> clogP$_{oct}$ 6). A possible rationale for this behaviour is presented in Figure 6, which depicts the compartments of the two experimental techniques. For the *in vitro* permeability experiment the apical and basolateral compartments are both aqueous environments where the free fraction is unity, since no protein is added to either reservoir. Compounds in the clogP$_{oct}$ range 2 to 4 are able to partition sufficiently into both membranes and the aqueous environment, such that the drug is first able to enter the cell membrane and then favourably partition out again into the aqueous basolateral compartment. With increasing lipophilicity there is a reduced driving force for the compound to partition back into the aqueous media *in vitro*, or alternatively, a greater significance of the unstirred water layer (Braun *et al.*, 2006). This latter effect was minimised by the experimental design of the *in vitro* permeability experiment. In addition, no correlation was observed between recovery

and lipophilicity (data not shown), highlighting that the trends in Figure 1b are likely

to be the result of the physicochemical characteristics of the drug.

In contrast to *in vitro* models, the *in situ* perfusion experiment is characterised by a

protein free perfusate (i.e. fu = 1) but a brain compartment where tissue binding may

occur, i.e. fu(brain). Flow limited uptake into the CNS appears to occur around a

clogP$_{oct}$ of ca. 2 and hence P becomes relatively insensitive to further increases in

lipophilicity. Therefore at high lipophilicities (clogP$_{oct}$ > 4), the brain tissue binding

may be acting as a drug sink which then helps to maintain the diffusion gradient

across the BBB. This facilitates the brain penetration of lipophilic drugs that would

otherwise appear to be poorly permeable as in the *in vitro* system. Other differences

between the two systems may also play a part in the shapes of the distributions shown

in Figures 1 and 2, such as the volume of the acceptor compartment in the *in vitro*

assay. Also the *in vivo* brain tissue volume substantially surpasses that of the acceptor

chamber in the *in vitro* system. For the most hydrophilic drugs present in the set

(fu(brain) < 0.1) there is a linear correlation between Papp and P (R^2 = 0.82). Polli *et*

al. (2000) observed a similar trend between rat *in situ* brain perfusion (Kin) and the

apparent permeability (Papp) derived from MDCK type I cells. Here an initial rising

linear phase was followed by a plateau when comparing Papp and Kin. The majority

of the hydrophilic compounds in the set comprised the initial linear phase (R^2 = 0.86).

Additionally Lundquist *et al.* (2002) observed a linear correlation between brain

uptake index (BUI) and the permeability coefficient (Pe) derived from a passaged

bovine brain endothelial co-culture cell model for a range of pre-dominantly

hyprophilic molecules. An R^2 value of 0.86 was noted on the logarithm transformed

data.

Figures 3 and 4 also suggest that there is an intrinsic link between BBB permeability and brain tissue binding, and therefore *in vivo* measures are likely to be influenced by both factors. In the range of lipophilicities lower than a clogP$_{oct}$ of 1, it appears that passive membrane permeability plays a greater influence on uptake into the CNS, whereas the sink action of tissue binding becomes important for more lipophilic drug molecules. An additional factor that may influence discrepancies between Papp and P is the presence of active uptake mechanisms *in vivo* that are absent in the *in vitro* model. Gabapentin is recognised by the large neutral amino acid transporter at the BBB (Uchino *et al.*, 2002). In the absence of active uptake gabapentin has a relatively poor passive permeability (0.4×10^{-6} cm/s) suggesting it would be too hydrophilic to significantly cross the BBB, yet its P value is quite substantial (1.6×10^{-3} cm/s). Knowledge of fu(brain) provides a means to place *in vitro* Papp values into a context relative to *in situ* measurements of P. From the results presented in this analysis, the MDR1-MDCKII cell model in conjunction with brain tissue binding and brain permeability across the BBB appears to be a useful tool in helping to rationalise CNS drug disposition. Clearly, careful consideration should be made in the choice of cell model. Lundquist *et al.* (2002) demonstrated a poor correlation between brain uptake index (BUI) and the permeability coefficient (Pe) derived from the Caco-2 cell line. However, as Caco-2 cells express a number of enzymes and transporters not found in brain endothelium, this finding may not be too surprising. Conversely, MDCK cells have low expression of transporters and little metabolic activity (Braun *et al.*, 2000) and therefore offer a more neutral test bed for which to study passive permeation.

In summary, BBB permeability and brain tissue binding play important roles in the disposition of CNS drugs. As cautioned recently by several authors, the success of CNS compounds as therapeutics should be viewed in terms of BBB permeability, drug pharmacological profile at the target, as well as interaction with brain parenchyma (Lee *at al.*, 2001; Doran *et al.*, 2005; Summerfield *et al.*, 2006). Permeability appears to be an important factor for compounds characterised by low brain tissue binding (fu(brain > 0.1) and low lipophilicity (clogP$_{oct}$ < 1). Brain tissue binding becomes important with increasing lipophilicity and may act as sink to help maintain the diffusion gradient across the BBB. Eventually, however, further increases in fu(brain) do not realise further increases in uptake across the BBB due to flow limited distribution into the brain. This raises the notion that a more complete picture CNS disposition is gained by considering the role of fu(brain) together with a measure of BBB permeability such as Papp or P, and such approaches may serve to improve the selection of new chemical entities with optimal physicochemical properties for CNS disposition. Information on the potential for drug efflux at the BBB is a further factor to consider when placed in the context of the extent of brain tissue binding (Summerfield *et al.*, 2006). A recent physiologically based PK model was reported by Liu *et al.* (2006), which highlighted the dual role of P and fu(brain) in determining the rate of drug entry into the brain. These findings are consistent with the results reported in this study and may contribute to improved compound selection for CNS delivery.

Acknowledgements

References

Alavijeh MS, Chishty M, Qaiser MZ, Palmer AM. (2005) Drug metabolism and pharmacokinetics, the blood-brain barrier, and central nervous system drug discovery. NeuroRx 2:554-571.

Ardizzone TD, Bradley RJ, Freeman AM, Dwyer DS. (2001) Inhibition of glucose transport in PC12 cells by the atypical antipsychotic drugs risperidone and clozapine, and structural analogs of clozapine. Brain Res 923: 82-90.

Begley DJ (1999) Methods for determining CNS drug transport in animals In Brain Barrier Systems, Alfred Benzon Symposium 45 (Paulson O, Knudsen GM and Moos T, eds), Munksgaard, Copenhagen, pp 91-109.

Bodor N and Buchwald P (2003) Brain Targeted drug delivery. Am J Drug Deliv 1:13-26.

Braun A, Hammerle S, Suda K, Rothen-Rutishauser B, Gunthert M, Kramer SD and Wundedrli-Allenspach H (2000), Cell cultures as tools in biopharmacy. Eur J Pharm Sci 11: S51-60.

Chikhale EG, Ng KY, Burton P and Borchardt RT (1994), Hydrogen bonding potential as a determinant of the in vitro and in situ blood-brain barrier permeability of peptides. Pharm Res 11:412-419.

Chikhale EC, Chikhale PJ and Borchardt RT (1995), Carrier-mediated transport of the antitumour agent acivicin across the blood-brain barrier. Biochem Pharmacol 49: 941-945.

Clark DE (1999) Rapid calculation of polar molecular surface area and its application to the prediction of transport phenomena. 2. Prediction of blood-brain barrier penetration. J Pharm Sci 88: 815-821.

Cohen BE, Bangham AD. (1972) Diffusion of small non-electrolytes across liposome membranes. Nature 236: 173-174.

Cserr HF and Bundgaard M (1984), Blood-brain interfaces in vertebrates: a comparative approach. Am J Physiol 246:R277-R288.

Doran A, Obach RS, Smith BJ, Hosea NA, Becker S, Callegari E, Chen C, Chen X, Choo E, Cianfrogna J, Cox LM, Gibbs JP, Gibbs MA, Hatch H, Hop CECA, Kasman IN, LaPerle J, Lui J, Liu X, Logman M, Maclin D, Nedza FM, Nelson F, Olson E, Rahematpura S, Raunig D, Rogers S, Schmidt K, Spracklin DK, Szewc M, Trouman M, Tseng E, Tu M, van Deusen JW, Venkatakrishnan K, Walens G, Wang, EQ, Wong D, Yasgar AS, Zhang C (2005) The impact of P-glycoprotein on the disposition of drugs targeted for indications of the central nervous system: evaluation using the mdr1a/b knockout mouse model. Drug Metab Dispos 33:165-174.

Fenstermacher J, Gross P, Sposito N, Acuff V, Pettersen S, Gruber K. (1988) Structural and functional variations in capillary systems within the brain. Ann N Y Acad Sci 529: 21-30.

Fisher H, Gottschilich R, Seelig A. (1998) Blood-brain barrier permeation: Molecular parameters governing passive diffusion. J Membr Biol 165: 201-211.

Greenwood J, Luthert PJ, Pratt O and Lantos PL (1985), Maintenance of the integrity of the blood-brain barrier in the rat during an in situ saline-based perfusion. Neurosci Lett 56: 223-227.

Hansch C, Steward AR, Anderson SM and Bentley DL (1968) Parabolic dependence of drug action upon lipophilic character as revealed by a study of hypnotics. J. Med. Chem 11: 1-11.

Kalvass JC, Maurer TS (2002) Influence of non-specific brain and plasma binding on CNS exposure: implications for rational drug discovery. Biopharm Drug Dispos 23:327-338.

Lee G, Dallas S, Hong M, Bendayan R (2001) Drug Transporters in the Central Nervous System: Brain Barriers and Brain Parenchyma Considerations. Pharm Rev 53: 569-596.

Liu X, Tu M, Kelly RS, Chen C and Smith BJ (2004), Development of a computational approach to predict blood-brain barrier permeability. Drug Metab Dispos 32: 132-139.

Lui X, Smith BJ, Chen C, Callegari E, Becker SL, Chen X, Cianfrogna J, Doran AC, Doran SD, Gibbs JP, Hosea N, Liu J, Nelson FR, Szewc MA, van Deusen (2006), Use of a physiologically based pharmacokinetics model to study the time to reach brain equilibrium: An experimental analysis if the role of blood-brain barrier permeability, plasma protein binding, and brain tissue binding. J Pharmacol Exp Ther 313:1254-1262.

Lundquist S, Renftel M, Brillault J, Fenart L, Cecchelli R and Dehouck MP (2002), Prediction of drug transport through the blood-brain barrier in vivo: A comparison between two in vitro cell models. Pharm Res 19:976-981.

Mahar Doan KM, Humphreys JE, Webster LO, Wring SA, Shampine LJ, Serabjit-Singh CJ, Adkison KK, Polli JW (2002) Passive permeability and P-glycoprotein-mediated efflux differentiate central nervous system (CNS) and non-CNS marketed drugs. J Pharmacol Exp Ther 303: 1029-1037.

Meyer FP, Banditt P, Schubert A and Schöche J (1999) Lamotrigine Concentrations in Human Serum, Brain Tissue, and Tumor Tissue. Epilepsia 40:68–73.

30

Murakami H, Takanaga H, Matsuo H, Ohtani H, Sawada Y (2000) Comparison of blood-brain barrier permeability in mice and rats using in situ brain perfusion technique. Am J Physiol Heart Circ Physiol 279:H1022-1028.

Ohno K, Pettigrw KD, Rapoport SI (1979) Local cerebral blood flow in the conscious rat as measured with 14C-antipyrine, 14C-iodoantipyrine and 3h-nicotine. Stroke 10:62-67.

Pardridge WM, Triguero D, Yang J and Cancilla PA (1990) Comparison of in vitro and in vivo models of drug transcytosis through the blood-brain barrier. J Pharmacol Exp Ther 253:884-891.

Pardridge WM (1997) Drug delivery to the brain. J Cereb Blood Flow Metab 17: 713-731.

Polli JW, Humphreys, JE, Wring SA, Burnette TC, Read KD, Hersey A, Butina D, Bertolotti L, Pugnaghi F and Serabjit-Singh C (2000), A comparison of Madin-Darby canine kidney cells and bovine brain endothelial cells as a blood-brain barrier screen in early drug discovery, In Progress in the Reduction, Refinement and Replacement of Animal Experimentation (Balls M, van Zeller AM and Halder ME eds), Elsevier Science B.V., pp 271-289.

31

Smith QR (1996), Brain perfusion systems for studies of drug uptake and metabolism in the central nervous system, In Models for Assessing Drug Absorption and Metabolism (Borchardt RT, ed), Plenum press, New York, pp 285-307.

Smith QR, Ziylan YZ, Robinson PJ and Rapoport SI (1988), Kinetics and distribution volumes for tracers of different sizes in the brain plasma space. Brain Res 462:1-9.

Street JA, Hemsworth BA, Roach AG, Day MD (1979) Tissue levels of several radio labelled beta-adrenoceptor antagonists after intravenous administration in rats. Arch Int Pharmacodyn Ther 237:180-190.

Summerfield SG, Stevens AJ, Cutler L, del Carmen Osuna M, Hammond B, Tang SP, Hersey A, Spalding DJ, Jeffrey P (2006), Improving the in vitro prediction of in vivo central nervous system penetration: integrating permeability, P-glycoprotein efflux, and free fractions in blood and brain. J Pharmacol Exp Ther 316:1282-1290.

Takada Y, Vistica DT, Grieg NH, Purdon D, Rapoport SI and Smith QR (1992) Rapid high-affinity transport of a chemotherapeutic amino acid across the blood-brain barrier. Cancer Res 52:2191-2196.

Takasato Y, Rapaport SI. Smith QR. (1984) An in situ brain perfusion technique to study cerebrovascular transport in the rat. Am J Physiol Heart Circ Physiol 247:H484-493.

Tamai I, Tsuji A, (2000) Transporter-mediated permeation of drugs across the blood-brain barrier. J Pharm Sci 89:1371-1388.

Terasaki T, Pardridge WM. (2000) Targeted drug delivery to the brain; (blood-brain barrier, efflux, endothelium, biological transport), J Drug Target 8:353-5.

Uchino H, Kanai Y, Kim do K, Wempe MF, Chairoungdua A, Morimoto E, Anders MW, Endou H. (2002) Transport of amino acid-related compounds mediated by L-type amino acid transporter (LAT1): Insights into the mechanisms of substrate recognition. Mol Pharmacol 61: 729-737.

Wang Q, Rager JD, Weinstein K, Kardos P, Dobson GL, Li J, Hidalgo IJ (2005) Evaluation of the MDR-MDCK cell line as a permeability screen for the blood-brain barrier. Int J Pharm 288: 349-359.

Woods HF and Youdim MBH (1978) The isolated perfused rat brain preparation - a critical assessment. Essays Neurochem Neuropharmacol 2:49-69.

Youdim KA, Qaiser MZ, Begley DJ, Rice-Evans CA, Abbott NJ (2004) Flavonoid permeability across an in situ model of the blood-brain barrier. Free Radic Biol Med 36:592-604.

Zlokovic BV, Begley DJ, Djuricic BM, Mitrovic DM (1986) Measurement of solute transport across the blood-brain barrier in the perfused guinea pig brain: method and application to N-methyl-alpha-aminoisobutyric acid. J Neurochem 46:1444-1451.

Legends for Figures

Figure 1: (a) Graph showing the relationship between fu(brain) and lipophilicity (cLog P_{oct}). Regression analysis ($Y = 0.7656X^{-0.4462}$, $R^2 = 0.638$) includes P-gp-substrates ($\square$, *in vitro* efflux ratio ≥ 3) and P-gp non-substrates ($\blacklozenge$), (b) Graph showing the relationship between passive membrane permeability from MDR1-MDCK assay and lipophilicity (cLog P_{oct}).

Figure 2: Graph showing the relationship between permeability surface product (P) and lipophilicity (cLog P_{oct}) for P-gp-substrates ($\square$, *in vitro* efflux ratio ≥ 3) and P-gp non-substrates ($\blacklozenge$).

Figure 3: Graph showing the relationship between passive permeability (Papp in presence of GF120918) and permeability surface product (P). Group A (denoted as $\blacksquare$) are characterised by clog $P_{oct} \geq 3$. Group B (denoted as ($\blacktriangle$) are characterised by clog $P_{oct} < 3$.

Figure 4: (a) Graph showing the relationship between lipophilicity (cLog P) and P/Papp. Regression analysis ($Y = 72.109 \times [P_{oct}]^{0.3145}$, $R^2 = 0.46$) includes P-gp-substrates ($\square$, *in vitro* efflux ratio ≥ 3) and P-gp non-substrates ($\blacklozenge$), (b) graph showing the relationship between fu(brain) and P/Papp. Regression analysis ($Y = 73.739 \times [P_{oct}]^{-0.6407}$, $R^2 = 0.73$) includes P-gp-substrates ($\square$) and P-gp non-substrates ($\blacklozenge$).

Figure 5: Plot of passive membrane permeability against permeability surface product (P) for compounds where fu(brain) > 0.1 (regression analysis, $Y = 0.0392X^{1.4076}$, $R^2 =$

0.82). Gabapentin has been omitted from the correlation (denoted by ♦) as an outlier,

possibly due to interaction with BBB transporters (Uchino et al., 2002).

Figure 6: Comparison of the compartments and barriers between *in situ* brain

perfusion and *in vitro* BBB model, such as MDR1-MDCK. Free fraction in each

compartment is denoted by fu.

Table 1: Data summary for marketed drug set showing several CNS related parameters, lipophilicity (clogP), free fraction in brain tissue homogenate (fu(brain)), passive membrane permeability in the MDR1-MDCK cell system in the presence of elacridar (Papp), *in vitro* P-gp efflux ratio (ER) and P/Papp. A P value could not be assigned to primidone due to no quantifiable concentrations measurable in the brain samples.

Compound Name	clogP$_{oct}$	fu(brain)		P (10-3 cm/s)		Papp A-B (10-6 cm/s)		Efflux Ratio	P/Papp
		Mean	SD	Mean	SD	Mean	SD		
Amantadine	2.20	0.2330	0.0350	0.77	0.13	7.1	0.2	0.8	162.5
Amitriptyline	4.90	0.0090	0.0010	21.43	2.93	9.8	1.2	**1.9**	3286.6
Amoxapine	2.40	0.0100	0.0040	17.86	1.07	14.8	1.1	4.1	1815.8
Atomoxetine	3.30	0.0190	0.0060	12.86	3.60	15.7	1.9	3.4	1229.4
Buproprion	3.50	0.1710	0.0270	10.13	1.00	47.5	2.2	1.4	319.9
Carbamazepine	2.70	0.1185	0.0070	6.40	1.40	30.9	1.7	**0.8**	310.6
Chlorpromazine	5.20	0.0020	0.0004	17.40	4.07	7.4	1.1	**0.8**	3551.0
Citalopram	2.50	0.0490	0.0040	3.87	0.67	18.1	3.5	20.1	321.2
Clozapine	3.50	0.0110	0.0010	15.07	1.33	28.3	2.2	1.3	798.5
Diazepam	3.00	0.0360	0.0050	13.15	3.07	46.4	1.8	1.0	425.3
Donepezil	4.70	0.1260	0.0150	10.54	2.53	33.8	1.5	2.3	468.4
Doxepin	3.90	0.0250	0.0030	14.61	2.73	16.3	1.3	1.9	1344.0
Ergotamine	3.60	0.0128	0.0022	3.30	0.87	10.2	1.2	49.6	485.6
Ethosuximide	0.40	0.7304	0.2273	1.33	0.20	9.7	0.3	0.8	30.8
Fluoxetine	4.10	0.0040	0.0010	17.99	2.27	6.4	1.1	**1.2**	4196.5
Fluphenazine	4.80	0.0009	0.0002	4.92	0.40	3.5	0.8	2.3	2127.8
Gabapentin	1.20	0.782	0.149	1.09	0.07	0.4	0.1	0.8	4188.0
Haloperidol	3.00	0.0110	0.0007	11.19	0.67	28.6	4.7	1.3	586.7
Isocarboxazid	1.00	0.2110	0.0380	16.36	3.93	17.7	7.4	1.2	1383.5

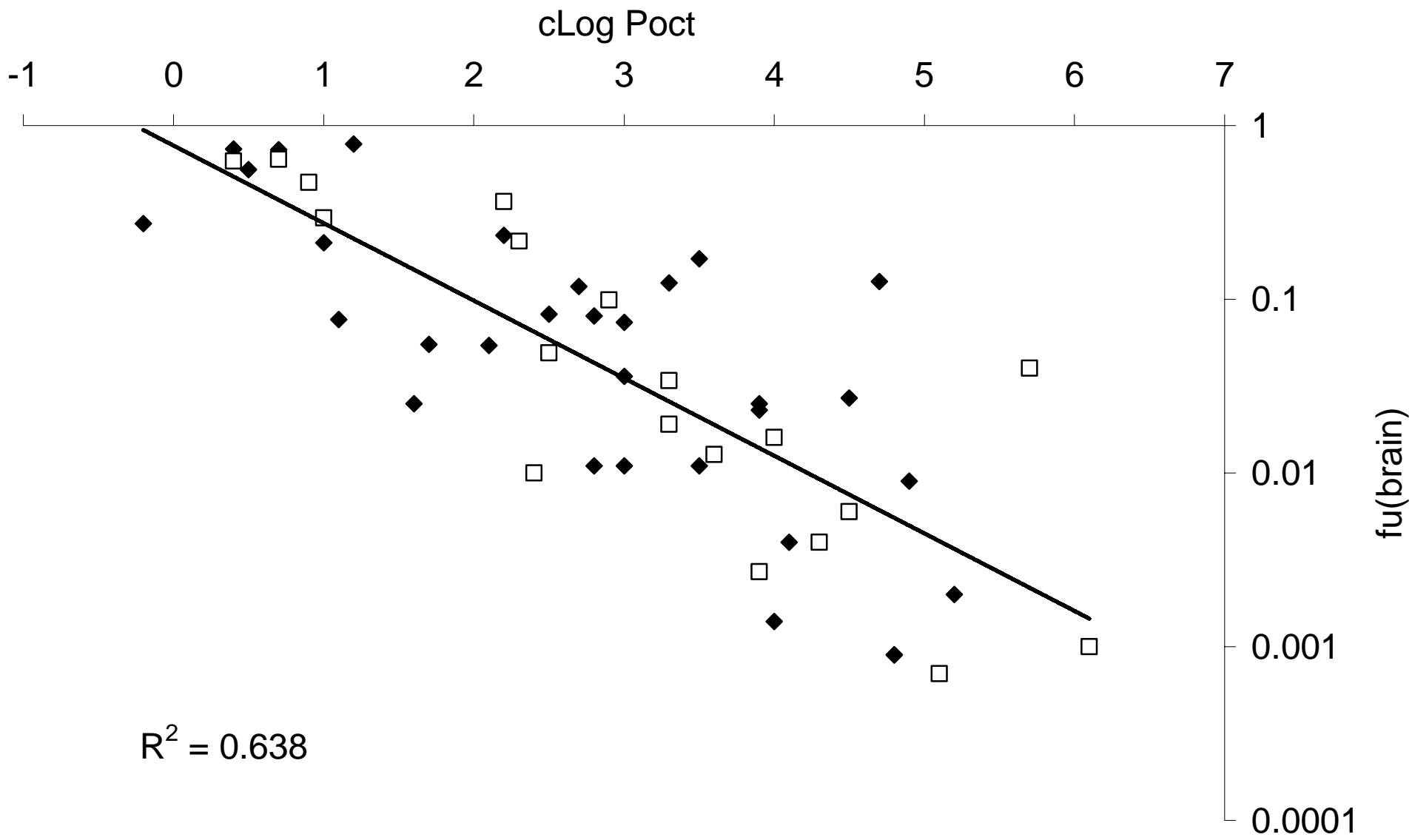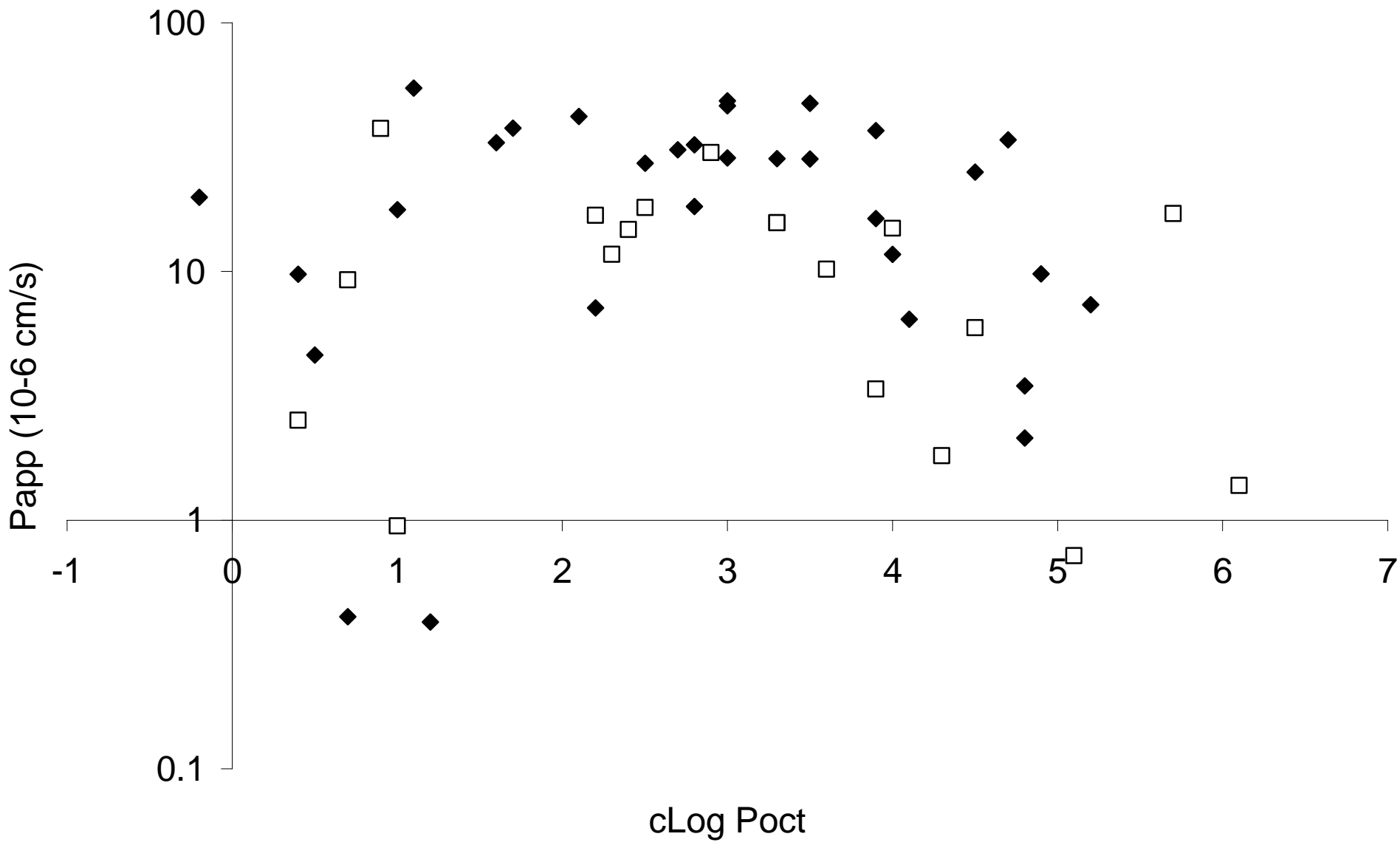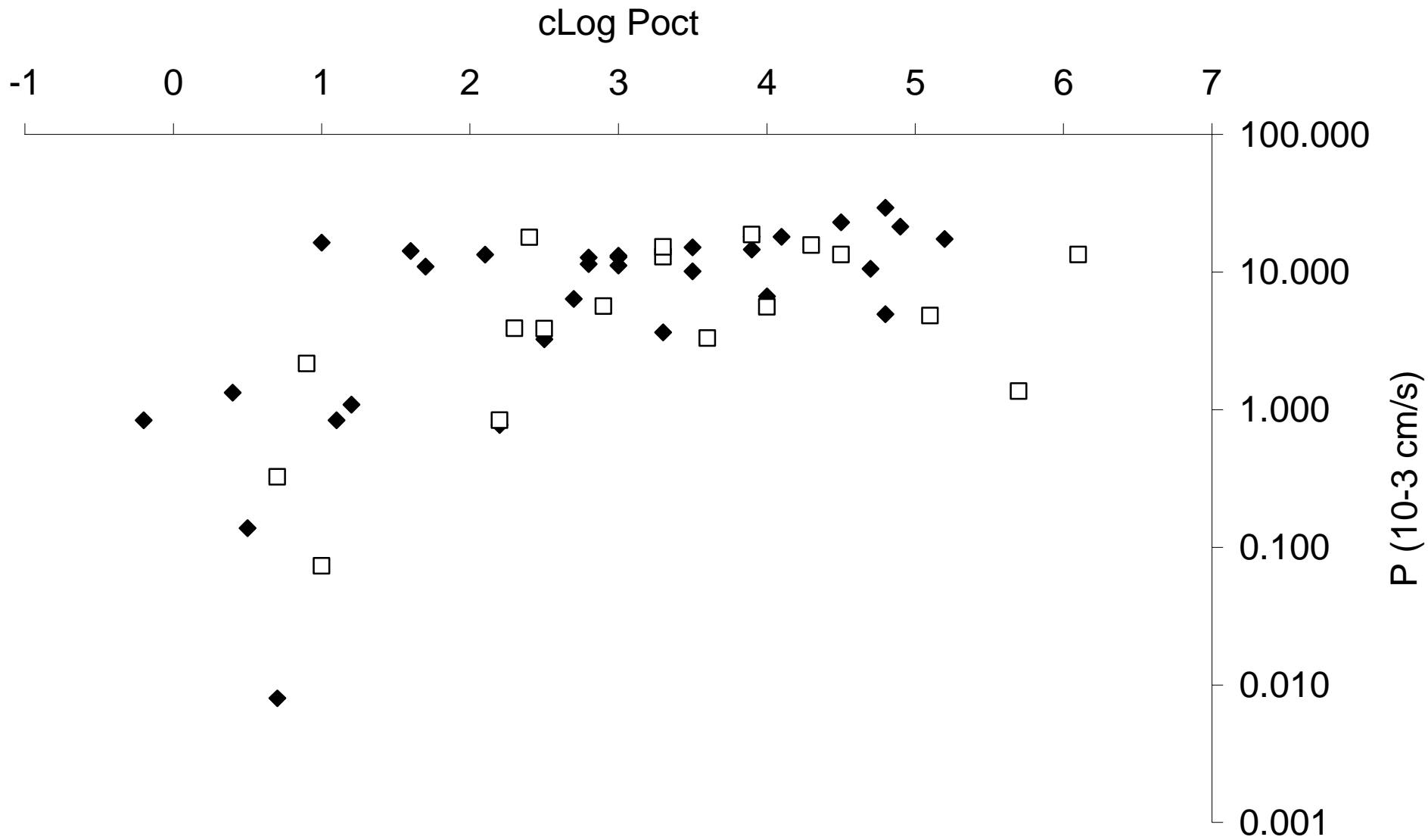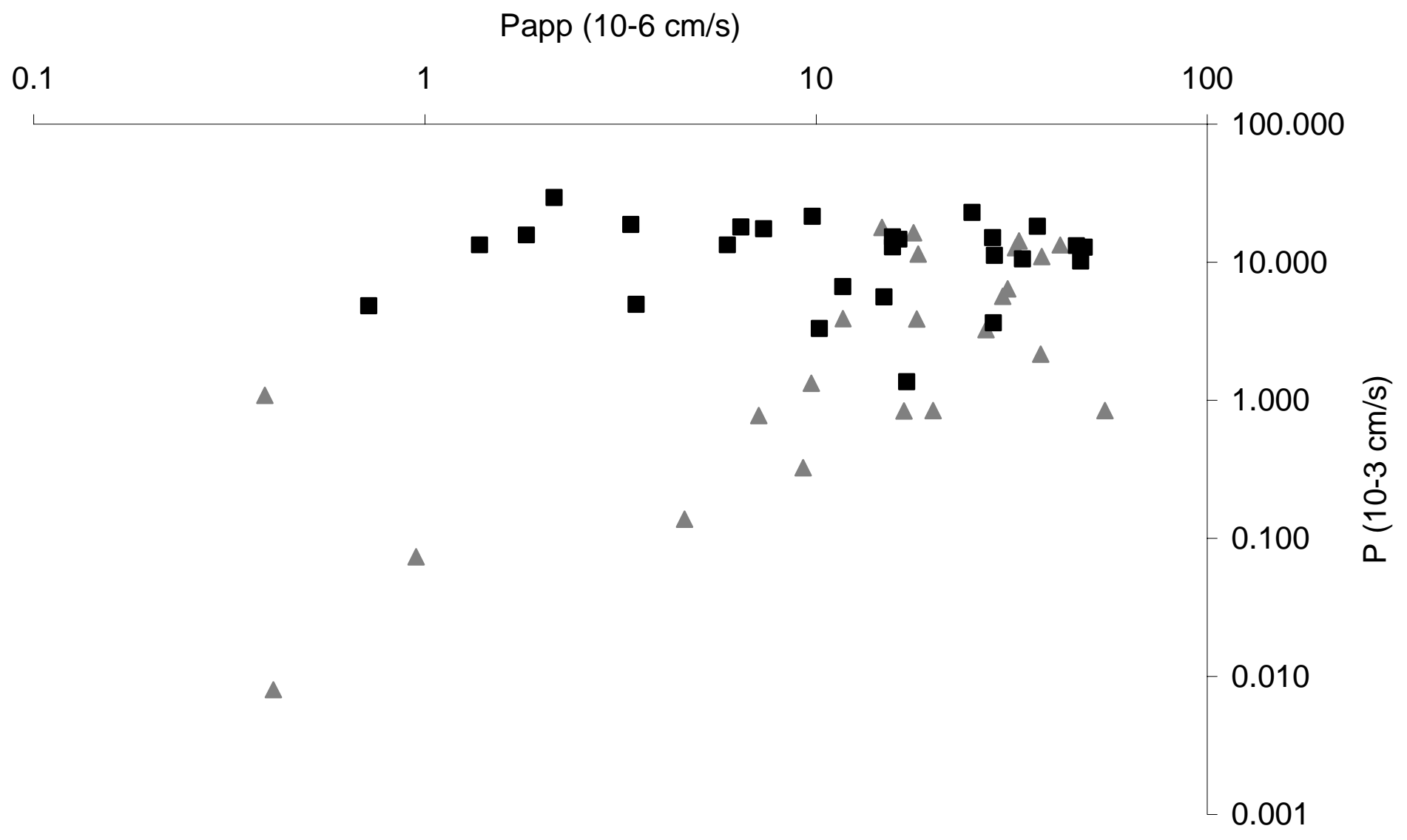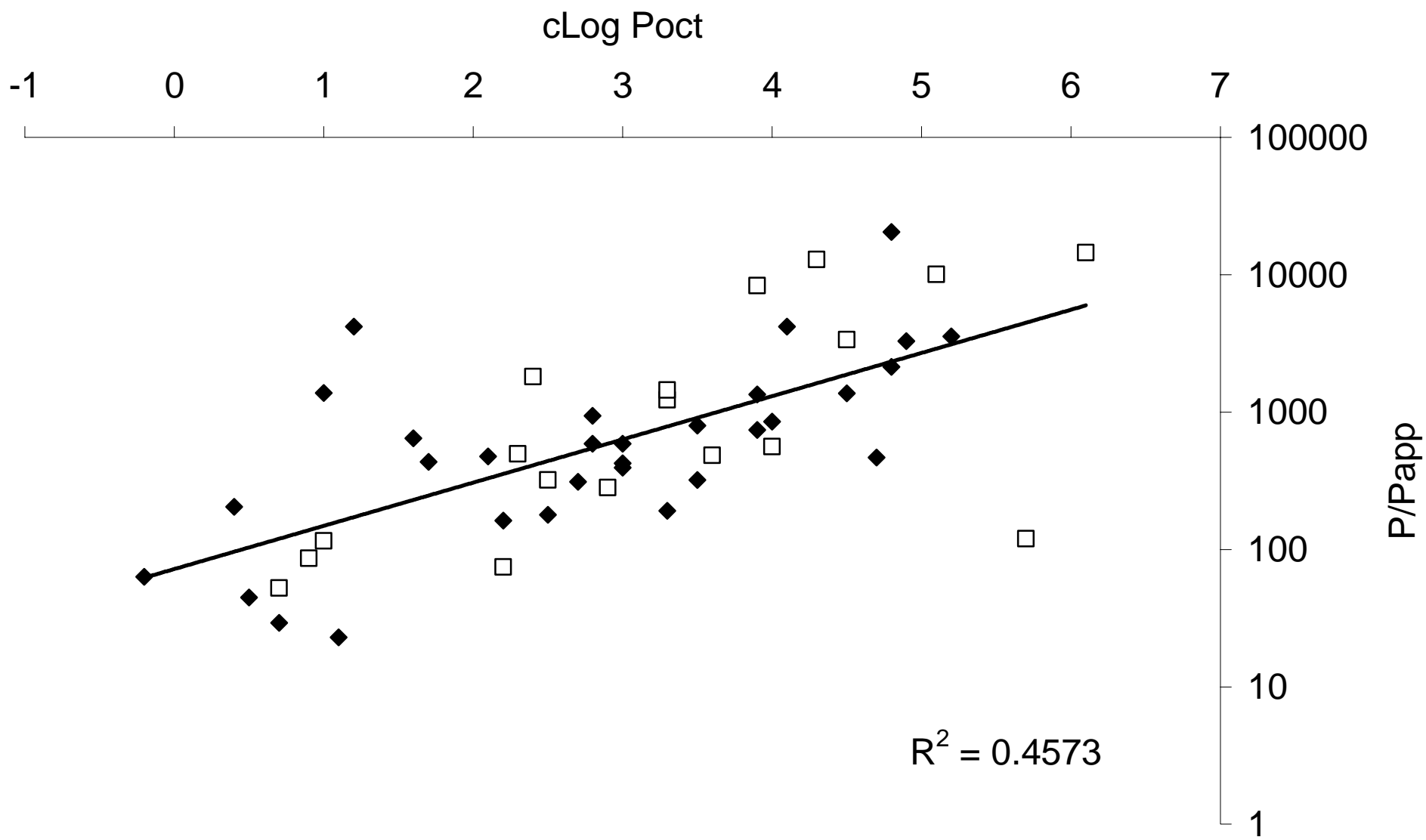|								
Lamotrigine	-0.20	0.2730	0.0340	0.84	0.05	19.9	1.7	1.6	63.3
Loxapine	2.80	0.0110	0.0030	11.41	2.27	18.2	1.6	1.2	938.9
Maprotiline	4.50	0.0060	0.0027	13.33	3.33	5.9	1.4	4.0	3367.0
Meprobamate	0.70	0.6380	0.0730	0.32	0.07	9.3	1.7	3.3	52.6
Mesoridazine	4.00	0.0160	0.0010	5.58	0.87	14.9	4.3	87.1	561.2
Metoclopramide	2.20	0.3650	0.0520	0.84	0.13	16.8	0.5	13.2	74.6
Midazolam	3.90	0.0230	0.0004	18.18	3.73	36.8	6.4	2.0	741.3
Mirtazapine	2.80	0.0800	0.0030	12.75	5.00	32.4	5.5	1.3	590.9
Olanzapine	3.30	0.0340	0.0090	15.20	0.93	15.7	2.2	4.9	1453.2
Pemoline	0.50	0.5580	0.0840	0.14	0.00	4.6	0.4	1.2	44.8
Pergolide	4.50	0.0270	0.0040	22.94	5.87	25.1	2.4	1.8	1372.4
Perphenazine	4.30	0.0040	0.0002	15.71	1.60	1.8	0.5	4.7	12945.1
Phenelzine	1.10	0.0763	0.0148	0.84	0.13	54.7	3.3	1.4	23.0
Phenytoin	2.50	0.0820	0.0060	3.25	0.60	27.2	3.1	2.8	179.0
Primidone	0.40	0.6220	0.1370	-	-	2.5	0.3	3.6	0.0
Quetiapine	1.60	0.0250	0.0020	14.21	2.13	33.0	1.4	1.5	645.7
Risperidone	2.90	0.0990	0.0030	5.66	1.27	30.0	2.8	20.8	282.8
Rizatriptan	1.00	0.2930	0.0880	0.07	0.00	1.0	0.3	8.4	115.8
Selegiline	3.00	0.0736	0.0030	12.81	3.00	48.6	3.0	0.8	395.9
Sertraline	4.80	0.0009	0.0001	29.28	8.27	2.1	0.3	2.6	20524.9
Sumatriptan	0.70	0.7240	0.0690	0.01	0.01	0.4	0.1	2.9	29.3
Tacrine	3.30	0.1240	0.0400	3.63	1.27	28.4	3.0	1.1	191.7
Temazepam	2.10	0.0540	0.0040	13.33	1.53	42.1	3.2	1.6	475.3
Thioridazine	6.10	0.0010	0.0004	13.34	2.07	1.4	0.1	33.7	14497.6
Thiothixene	3.90	0.0027	0.0004	18.73	3.47	3.4	0.6	47.7	8360.1
Tiagabine	5.70	0.0400	0.0120	1.36	0.07	17.1	0.9	25.8	119.4
Trazodone	1.70	0.0550	0.0060	10.96	0.40	37.7	0.4	1.1	436.4
Trifluoperazine	5.10	0.0007	0.0001	4.82	0.93	0.7	0.1	7.3	10046.3
Venlafaxine	2.30	0.2160	0.0230	3.89	0.40	11.7	2.9	4.7	498.0
Zaleplon	0.90	0.4710	0.0440	2.16	0.40	37.5	1.7	5.6	86.2
Ziprasidone	4.00	0.0014	0.0001	6.65	0.73	11.7	1.3	1.7	853.0

37

Figure 1a

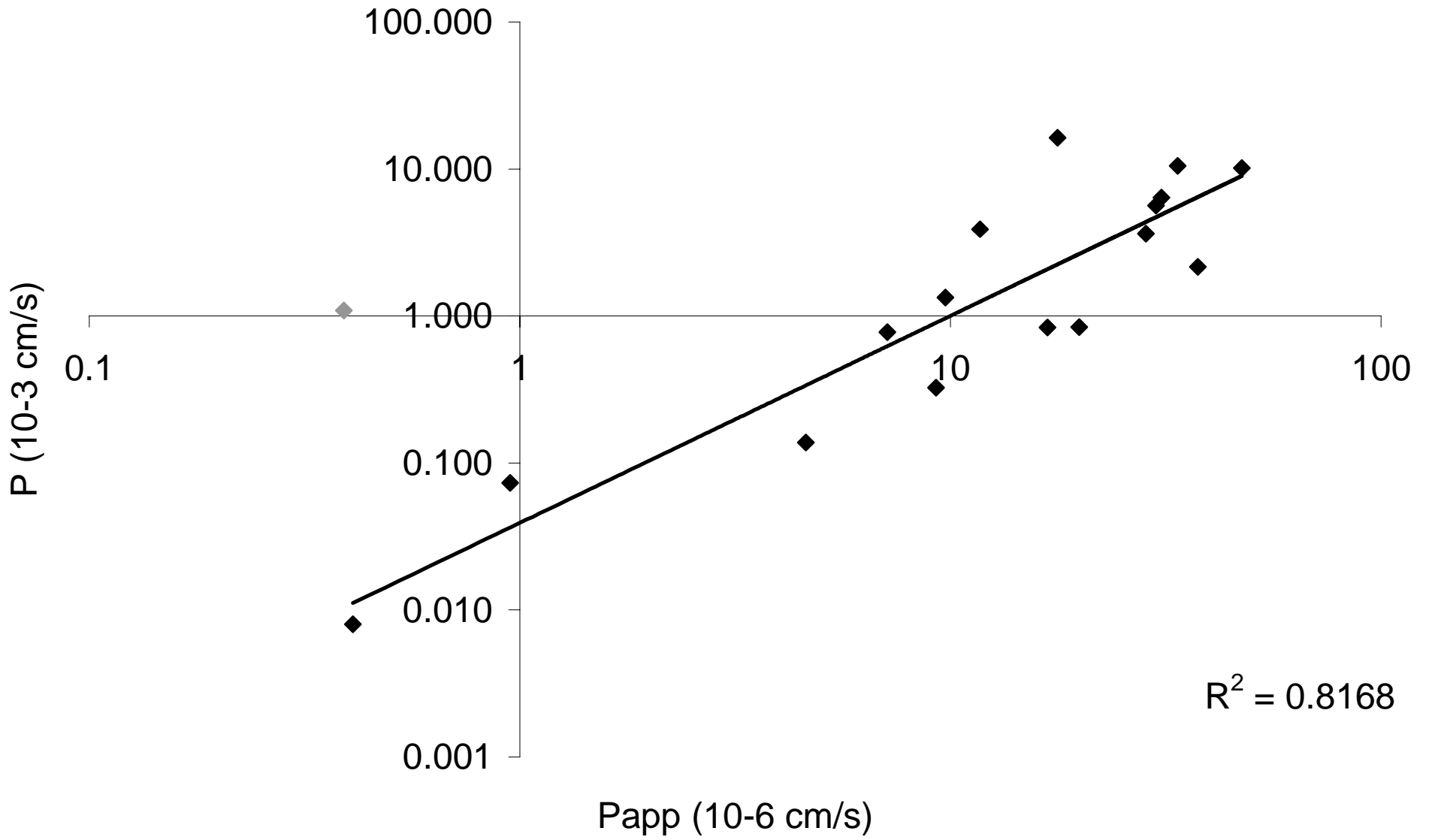Figure 1b

Figure 2

Figure 3

Figure 4a

Figure 4b

$R^2 = 0.8168$

Figure 5

in vitro MDCK cell layer

Apical

fu = 1

P-gp

Basolateral

fu = 1

---

in situ Rat BBB

P-gp

Perfusate

fu = 1

Other BBB
transporters

Brain

fu = fu(brain)

Figure 6